

51

Springer Series in Solid-State Sciences

Edited by Manuel Cardona

Phonon Scattering in Condensed Matter

Proceedings of the
Fourth International Conference
University of Stuttgart, Fed. Rep. of Germany
August 22-26, 1983

Editors:

W. Eisenmenger, K. Laßmann, and S. Döttinger

Phonon Scattering in Condensed Matter

Proceedings of the
Fourth International Conference
University of Stuttgart, Fed. Rep. of Germany
August 22-26, 1983

Editors:
W. Eisenmenger, K. Laßmann, and S. Döttlinger

With 321 Figures

Springer-Verlag
Berlin Heidelberg New York Tokyo 1984

Professor Dr. Wolfgang Eisenmenger

Dr. Kurt Laßmann

Dr. Siegfried Döttinger

Physikalisches Institut der Universität Stuttgart, Pfaffenwaldring 57

D-7000 Stuttgart 80, Fed. Rep. of Germany

Series Editors:

Professor Dr. Manuel Cardona

Professor Dr. Peter Fulde

Professor Dr. Hans-Joachim Queisser

Max-Planck-Institut für Festkörperforschung, Heisenbergstrasse 1

D-7000 Stuttgart 80, Fed. Rep. of Germany

Organizing Committee

Döttinger, S.; Dransfeld, K.; Eisenmenger W. (*Chairman*); Laßmann, K.; Sigmund, E.; Wagner, M.;

International Advisory Committee

Anderson, A. C. Urbana, USA

Bron, W. E. Bloomington, USA

Challis, L. J. Nottingham, UK

Cheeke, J. D. N. Sherbrooke, Canada

Dobbs, E. R. London, UK

Fossheim, K. Trondheim, Norway

de Goër, A. M. Grenoble, France

Ikushima, A. J. Tokyo, Japan

Ishiguro, T. Ibaraki, Japan

Joffrin, J. Paris, France

Kaplyanskii, A. A. Leningrad, USSR

Khalatnikov, I. M. Moscow, USSR

Kinder, H. Munich, FRG

Klemens, P. G. Connecticut, USA

Kopvillem, U. Vladivostok, USSR

Maneval, J. P. Paris, France

Maris, H. J. Providence, USA

Narayanamurti, V. New Jersey, USA

Renk, K. F. Regensburg, FRG

Shiren, N. S. New York, USA

Weis, O. Ulm, FRG

Weiss, K. Schaun, FL

Wyatt, A. F. G. Exeter, UK

ISBN 3-540-12954-5 Springer-Verlag Berlin Heidelberg New York Tokyo

ISBN 0-387-12954-5 Springer-Verlag New York Heidelberg Berlin Tokyo

This work is subject to copyright. All rights are reserved, whether the whole or part of the material is concerned, specifically those of translation, reprinting, reuse of illustrations, broadcasting, reproduction by photocopying machine or similar means, and storage in data banks. Under § 54 of the German Copyright Law, where copies are made for other than private use, a fee is payable to "Verwertungsgesellschaft Wort", Munich.

© by Springer-Verlag Berlin Heidelberg 1984

Printed in Germany

The use of registered names, trademarks, etc. in this publication does not imply, even in the absence of a specific statement, that such names are exempt from the relevant protective laws and regulations and therefore free for general use.

Offset printing: Beltz Offsetdruck, 6944 Hemsbach/Bergstr. Bookbinding: J. Schäffer OHG, 6718 Grünstadt, 2153/3130-54 3 210

Preface

This volume contains the proceedings of the Fourth International Conference on Phonon Scattering in Condensed Matter held from August 22-26, 1983 at the University of Stuttgart. The preceding conferences were organized at Saint Maxime and Paris in 1972, at the University of Nottingham in 1975, and at the Brown University Providence/Rhode Island in 1979.

The Stuttgart conference, like the preceding conferences, was mainly concerned with "propagating" high-frequency acoustic phonons, mechanical waves and heat up to the lattice limiting frequency. Lattice dynamics, optical phonons, phase transitions, etc., were included as far as they are involved in acoustical phonon scattering, propagation and generation. In this context the conference covered all aspects of acoustical phonon physics, especially generation of phonons, propagation, scattering and detection. Since acoustic phonons participate in most energy-transfer processes in solids and liquids, the field of interest is growing rapidly. Therefore exciting new developments of acoustic phonon physics could be presented at the Stuttgart conference as well as important progress with respect to well-known problems, as, for example, the Kapitza resistance.

Two hundred and six scientists from 21 countries attended the conference. Thirteen invited papers and 105 contributed papers, with 34 as posters, were presented. The discussions are included in this volume.

A discussion session on large wave vector phonons was organized and chaired by V. Narayanamurti. A discussion session on phonon scattering at interfaces was organized and chaired by R.O. Pohl.

The conference was supported and sponsored by the Deutsche Forschungsgemeinschaft, the International Union of Pure and Applied Physics, the Land Baden Württemberg, the University of Stuttgart, the Deutsche Physikalische Gesellschaft and the E. Leitz Company, Wetzlar. The support and sponsorship of these organizations is gratefully acknowledged.

We extend our thanks to the Rektor of the University of Stuttgart, Prof. Dr. rer. nat. H. Zwicker, who opened the conference and gave a reception for the delegates.

We should like to thank all members of the international advisory committee for their extremely helpful suggestions and recommendations.

We thank our colleagues of the organization committee K. Dransfeld, E. Sigmund and M. Wagner for close and fruitful cooperation. Special thanks are due to our colleague H.-J. Bauer for his advice and assistance in adapting our data handling system to the needs of the conference. In particular we thank Mrs. R. Mann, Mrs. I. Poljak and Mrs. G. Untereiner as well as all our co-workers and students for their invaluable assistance and help during all stages of the conference.

Stuttgart, December 1983

W. Eisenmenger · K. Laßmann · S. Döttinger

Contents

Part I. Acoustic Phonon Spectroscopy

*Crossing Effects in Phonon Scattering By L.J. Challis (With 10 Figures)	2
*Far Infrared Volume Generation and Detection of Phonons By K.F. Renk (With 5 Figures)	10
*The Josephson Junction—A New Tunable Phonon Source with High-Frequency Resolution. By P. Berberich and H. Kinder (With 5 Figures)	18
*Two Applications of Microwave Acoustics in Liquid Helium: High Resolution Microscopy and Direct Measurement of Phonon Dispersion By D. Rugar (With 5 Figures)	26
Heater Film Dynamics, Phonon Diffusion and Phonon Decay. By T.E. Wilson, W.E. Bron, F.M. Lurie, and W.L. Schaich (With 2 Figures)	34
Infrared Excitation of High-Frequency Phonons by Multiphonon Absorption By U. Happek, R. Baumgartner, and K.F. Renk (With 2 Figures)	37
Zero-Field Hyperfine Splitting of $Al_2O_3:V^{3+}$ by Josephson Phonon Spectroscopy. By A. Schick, P. Berberich, W. Dietsche, and H. Kinder (With 2 Figures)	40
Subnanosecond Bolometry Using Niobium Films By J.P. Maneval, J. Desailly, and B. Pannetier (With 2 Figures) ...	43
Generation of High-Frequency Phonons by Metallic Point Contacts By R.J.G. Goossens, A.G.M. Jansen, J.I. Dijkhuis, P. Wyder, and H.W. de Wijn (With 4 Figures)	46
Nonequilibrium Phonon Distribution in a Quantizing Magnetic Field: A Tunable GHz to THz Phonon Generator? By G.W. Slater and A.-M.S. Tremblay (With 3 Figures)	49
Relaxation Processes and Response Time of Superconductors to a Periodic Excitation. By C. Vanneste and N. Perrin (With 3 Figures)	52
Amplitude Modulated Heat Pulses By L. Hirschbiegel, M. Siemon, and W. Grill (With 2 Figures)	55

*invited paper

Thermal Conductivity Measurement Under Applied Uniaxial Stress By B. Salce (With 2 Figures)	58
Thin Piezoelectric PVDF-Layers as Ultrasonic Transducers. By A. Ambrosy, K. Holdik, W. Scheitler, and H. Schulze (With 7 Figures)	61
Discussions	64

Part II Phonon Focusing

Phonon Focusing in Germanium Imaged by Electron-Beam Scanning By W. Metzger, R. Eichele, H. Seifert, and R.P. Huebener (With 3 Figures)	72
Nonlinear Phonon Focusing. By D. Armbruster, G. Dangelmayr, and W. Güttinger (With 7 Figures)	75
Phonon Focusing in Highly Dispersive and Isotopically Impure Crystals By S. Tamura (With 4 Figures)	78
Spatial Variation of Phonon Distribution in Thermal Conduction By F.W. Sheard, G.A. Toombs, and S.R. Williams (With 2 Figures) ...	81
Discussions	84

Part III Large Wave-Vector Phonons

Observation of a Quasi-Diffusive Phonon Propagation Mode. By W.E. Bron, J.M. O'Connor, and Y.B. Levinson (With 2 Figures)	88
Propagation of Near Zone Boundary Acoustic Phonons in Solid (hcp) ^4He By T. Haavasoja, V. Narayanamurti, and M.A. Chin (With 4 Figures) .	91
Scattering of Debye Phonons by Substitutional Defects in Solids By V.P. Srivastava	94
Direct Observation of Ballistic Large-Wavevector Phonon Propagation in Gallium Arsenide. By B. Stock, R.G. Ulbrich, and M. Fieseler (With 2 Figures)	97
Search for Large k-Vector Phonons in GaAs By J.P. Wolfe and G.A. Northrop (With 3 Figures)	100
On the Propagation of Long-Lived Short Wavelength TA Phonons in GaAs By M. Lax, V. Narayanamurti, R. Ulbrich, and N. Holzwarth (With 4 Figures)	103
Temperature Dependence of Optical Phonon Lifetimes. By J. Kuhl, B.K. Rhee, and W.E. Bron (With 2 Figures)	106
Anharmonic Decay of High-Energy LA Phonons By S. Tamura and K. Okubo (With 3 Figures)	109
Lifetime and Linewidth of Resonant 40-cm^{-1} Phonons in Alexandrite By R.J.G. Goossens, J.I. Dijkhuis, and H.W. de Wijn (With 3 Figures)	112

High-Frequency Phonon Dynamics in LaF_3 Using Monoenergetic Optical Detection Methods. By R.S. Meltzer, J.E. Rives, D.J. Sox, and G.S. Dixon (With 3 Figures)	115
Raman Spin-Lattice Relaxation Induced by Optically Generated Zone-Boundary Phonons in Ruby. By J.G.M. van Miltenburg, J.I. Dijkhuis, and H.W. de Wijn (With 2 Figures)	118
Raman Probe of the Brillouin Zone for Nonequilibrium Phonons in GaAs By R. Bray, K.T. Tsen, and K. Wan (With 1 Figure)	121
Phonon Decay in X-Ray Irradiated Ruby Crystals By M. Engelhardt and K.F. Renk (With 4 Figures)	124
Decay of a Highly Excited Phonon Mode By P. Ullersma (With 1 Figure)	127
Stimulated Emission and Decay of Phonons Resonant Between the Zeeman States of $\bar{E}(^2E)$ in Ruby. By J.G.M. van Miltenburg, G.J. Jongerden, J.I. Dijkhuis, and H.W. de Wijn (With 3 Figures)	130
Raman Scattering and the Two-Phonon Density of States in GaAs By M. Lax, V. Narayanamurti, R.C. Fulton, R. Bray, K.T. Tsen, and K. Wan (With 2 Figures)	133
Propagation of Phonons Generated by Nonradiative Transitions in KCl-NO_2 By I. Sildos, G. Zavt, and I. Dolindo (With 2 Figures)	136
Discussions	139

Part IV Surfaces, Interfaces, Kapitza Resistance

*Phonon-Induced Desorption of Helium By P. Taborek (With 4 Figures)	148
*Thermal Boundary Resistance Between Small Particles and Liquid He-3 By T. Nakayama (With 5 Figures)	155
*Scattering and Absorption of Ballistic Phonons by the Electron Inversion Layer in Silicon: Theory and Experiment. By J.C. Hensel, R.C. Dynes, B.I. Halperin, and D.C. Tsui (With 6 Figures)	163
*Low Wavevector Phonons in the 2-Dimensional Electron Solid on Liquid Helium. By F.I.B. Williams (With 5 Figures)	171
Reciprocity Theorem for Phonon Transitions at Ideal Interfaces Within the Acoustic Mismatch Model. By O. Weis (With 3 Figures)	179
Phonon Scattering by Twin Planes By J.W. Vandersande, P.N. Chopra, and R.O. Pohl (With 3 Figures) ..	182
Boundary and Dislocation Scattering of Phonons in Lead Single Crystals By W. Odoni, P. Fuchs, and H.R. Ott (With 2 Figures)	185
Diffuse Scattering of Thermal Phonons at Crystal Surfaces By T. Klitsner and R.O. Pohl (With 2 Figures)	188

*invited paper

Imaging of Specularly Reflected Phonons from a Crystal Boundary By G.A. Northrop (With 2 Figures)	191
Critical-Cone Channeling of Thermal Phonons from Solid/Solid Interfaces By A.G. Every, G.L. Koos, G.A. Northrop, and J.P. Wolfe (With 2 Figures)	194
Anomalous Low Temperature Kapitza Resistance of a Paramagnetic Salt By G.J. Batey and P.C. Main (With 3 Figures)	197
A Size Effect in the Kapitza Resistance to Dilute ^3He - ^4He Mixtures By F. Guillon, J.P. Harrison, and A. Sachrajda (With 2 Figures) ...	200
Kapitza Resistance Near 1 mK—The Shaking Box Model. By A.R. Rutherford, J.P. Harrison, and M.J. Stott (With 2 Figures)	203
Phonon and Roton-Induced Evaporation. By A.P.G. Wyatt, M.J. Baird, and F.R. Hope (With 4 Figures)	206
Spectral Dependence of the Kapitza Resistance Between 0.5 K and 2.3 K By O. Koblinger, E. Dittrich, U. Heim, M. Welte, and W. Eisenmenger (With 3 Figures)	209
Kapitza Resistance of Laser-Annealed Surfaces. By H.C. Basso, W. Dietsche, H. Kinder, and P. Leiderer (With 2 Figures)	212
Discussions	215

Part V Quantum Liquids and Crystals

*Crystallization Waves in Helium. By A. Ya. Parshin (With 6 Figures)	226
*Phonon Transmission and the Kapitza Resistance Between Liquid and Solid Helium. By H.J. Maris (With 7 Figures)	234
*Transmission of Sound at the Solid-Liquid Interface of ^4He By B. Castaing, L. Puech, and G. Bonfait (With 3 Figures)	241
Propagation of High Frequency Phonons in Liquid He II. By T. Haavasoja, V. Narayanamurti, and M.A. Chin (With 4 Figures)	249
Ultrasonic Attenuation in $\text{KCl}:\text{OH}^-$ with High OH Concentration By M. Saint-Paul, R. Nava, and J. Joffrin (With 2 Figures)	252
Localized Phonon Mode Associated with Dislocations in Alkali Halide Crystals. By Y. Hiki, Y. Kogure, and F. Tsuruoka (With 3 Figures) .	254
^3He - ^3He Interaction in ^3He - ^4He Liquid Mixtures Determined from Sound Attenuation. By A.J. Ikushima, I. Fujii, M. Fukuhara, and K. Kaneko (With 2 Figures)	257
Ultrasonic-Attenuation and Pressure Measurements in Phase-Separated Solid ^3He - ^4He Mixtures By I. Iwasa and H. Suzuki (With 2 Figures)	260

*invited paper

Effects of Anharmonicities and Broken Time-Reversal Invariance on Static and Dynamic Properties of Two-Dimensional Electron Solids By G. Meissner (With 1 Figure)	263
Charge-Induced Deformation of the ^4He Solid-Superfluid Interface By J. Bodensohn, P. Leiderer, and D. Savignac (With 2 Figures)	266
Pinning of Dislocations in Helium by Large Ultrasonic Stresses By J.R. Beamish and J.P. Franck (With 1 Figure)	269
Discussions	272

Part VI Cooperative Phenomena

Ultrasonic Velocity and Attenuation Near the Cooperative Jahn-Teller Dilation in Cerium Ethyl Sulphate By J.T. Graham and J.H. Page (With 2 Figures)	278
Ultrasonic Attenuation at Megahertz Frequencies in the Cooperative Jahn-Teller System TmVO_4 . By J.H. Page and S.R.P. Smith (With 3 Figures)	281
Thermoelectric Power of $\text{TiSe}_2\text{-xSx}$ Mixed Crystals. By A.A. Lakhani, S. Jandl, J.P. Jay-Gerin, and C. Ayache	284
Ultrasonic Study of Melting of Crystalline Solids By Y. Hiki and J. Tamura (With 3 Figures)	285
Piezoeacoustic Observation of Acoustic Soft Mode in KH_2PO_4 Crystal By J.Y. Koo, T.W. Yoo, and J.J. Kim (With 3 Figures)	288
Brillouin-Scattering Study of Sound Velocity of Quartz at α - β Transition. By H. Unoki, H. Tokumoto, and T. Ishiguro (With 2 Figures)	292
Phonon-Soliton Interaction in K_2SeO_4 By W. Rehwald (With 3 Figures)	296
Thermal Conductivity of Cooperative Jahn-Teller E- b_1, b_2 Systems By W. Mutscheller and M. Wagner (With 2 Figures)	298

Part VII Free Carriers

Magnetic Field Dependence of Ultrasonic Attenuation in Heavily Doped Ge:Sb. By H. Sakurai, K. Suzuki, and T. Miyasato (With 2 Figures)...	302
Phonon Attenuation in Heavily Doped p-Type Semiconductors By T. Sota, K. Suzuki, and D. Fortier (With 2 Figures)	304
Ballistic Phonon Transport in Ge:P Under Magnetic Field By T. Miyasato, M. Tokumura, and K. Suzuki (With 4 Figures)	307
Hole-Phonon Interaction in Wurtzite-Type Semiconductors By M. Singh and J. Leotin (With 2 Figures)	310

The Observation of Strongly Coupled Magnetic Ions in Al_2O_3 by Low Temperature Thermal Expansion Measurements By I.J. Brown and M.A. Brown (With 2 Figures)	313
Sound Velocity Measurements in Highly Oriented and Intercalated Graphite Specimen by Direct Electromagnetic Excitation of Ultrasound. By K. de Groot, V. Müller, D. Maurer, V. Geiser, and H.-J. Güntherodt (With 3 Figures)	316
The Effect of Electron Relaxation on Damping of Long-Wavelength Phonons in Metals and Heavily Doped Semiconductors. By I.P. Ipatova, A.V. Subashiev, and V.A. Shchukin (With 1 Figure)	319
Nuclear Acoustic Resonance Measurements of the Electron-Phonon Interaction in bcc Transition Metals. By V. Müller, E.-J. Unterhorst, and W. Neumann (With 3 Figures)	322
Revision of the Statistical Mechanics of Phonons to Include Phonon Linewidths. By W.C. Overton Jr. (With 1 Figure)	325
Phonon Emission and Electron Heating in a Two-Dimensional Electron Gas By M.A. Chin, V. Narayanamurti, H.L. Stormer, and J.C.M. Hwang (With 4 Figures)	328
Density and Field Dependence of the Phonon-Limited Hot-Electron Temperature in n-Si Inversion Layers. By R.A. Höpfel, E. Vass, and E. Gornik (With 2 Figures)	331
Amplification of Total-Reflection-Mode Surface Phonons in n-Type InSb Films. By Cr-C. Wu (With 3 Figures)	335
Time-Resolved Photoluminescence and Phonon Transport in Amorphous Si:H Films. By U. Strom, J.C. Culbertson, P.B. Klein, and S.A. Wolf (With 3 Figures)	338
Surface Acoustic Waves in Metals. By J. Heil, I. Kouroudis, C. Lingner, and B. Lüthi (With 2 Figures)	341
Discussions	344

Part VIII Defects

*Phonon Scattering by Dislocations. By A.C. Anderson (With 4 Figures) ..	348
The Acoustic Paramagnetic Resonance of Cr^{2+} in n-Type GaAs By A.S. Abhiani, C.A. Bates, P.J. King, D.R. Pooler, V.W. Rampton, P.C. Wiscombe, and P. Bury (With 1 Figure)	355
Magnetic-Field-Dependent Phonon Scattering by Li Ions in Si By L.J. Challis, A.P. Heraud, V.W. Rampton, M.K. Saker, and M.N. Wybourne (With 2 Figures)	358
Influence of Defects on the Splitting of the Acceptor Ground State in Silicon. By A. Ambrosy, A.M. de Goër, K. Laßmann, B. Salce, and H. Zeile (With 4 Figures)	361
Phonon Scattering at Electronically Degenerative Systems: An Application to the Defect Systems Si(In), Si(B), and GaAs (Mn) By J. Maier and E. Sigmund (With 6 Figures)	364

*invited paper

Magnetothermal Conductivity of Boron-Doped-Silicon By L.J. Challis and A.P. Heraud (With 2 Figures)	368
An Additive Conservation Law for Phonon Collision Operator in Molecular Crystals. By B. Perrin (With 2 Figures)	371
Discussions	374

Part IX Two-Level Systems

*Low-Energy Excitations in Disordered Solids: New Aspects By S. Hunklinger (With 3 Figures)	378
Anomalous Low-Temperature Ultrasonic Behaviour in a Fluoride Glass Containing Mn. By P. Doussineau, A. Levelut, M. Matecki, and W.D. Wallace (With 2 Figures)	386
Vibrational Dynamics of Lithium Ions in β -Alumina Crystals By R. Di Valerio, A. Fontana, G. Mariotto, and M. Montagna (With 4 Figures)	389
Low-Energy Excitations in $(\text{KBr})_{1-x}(\text{KCN})_x$ in the Orientational Glass State. By M. Meissner, J.J. de Yoreo, R.O. Pohl, and S. Susman (With 2 Figures)	392
Spectral Hole Burning of Dyes, Probing Phonon Processes at Surfaces and in Amorphous Systems. By U. Bogner and G. Röska (With 2 Figures) ..	395
Evidence of Two-Level Systems in Electrolyte Glass by Brillouin Scattering. By J. Pelous, R. Vacher, A. Essabouri, U. Reichert, and M. Schmidt (With 2 Figures)	398
Acoustic Absorption Due to Hydrogen Tunneling in $\text{NbNb}_{0.0015}\text{H}_{0.0025}$ By J.L. Wang, G. Weiss, H. Wipf, and A. Magerl (With 1 Figure)	401
Phonon Scattering in Phosphorous-Implanted Silicon By M. Grimshaw and G. Feuillet (With 1 Figure)	404
Relaxation Ultrasonic Attenuation Measurements in Quartz Slightly Disordered by Neutron Irradiation. By C. Laermans and V. Esteves (With 2 Figures)	407
Low-Energy Excitations in Zr-Based Amorphous Alloys Studied by Thermal Conductivity and Specific Heat. By J.C. Lasjaunias, A. Ravex, and O. Bèthoux (With 3 Figures)	410
Low-Temperature Thermal Properties of Amorphous $\text{Zr}_x\text{Cu}_{1-x}$ After Structural Relaxation. By H.J. Schink, S. Grondy, H. v. Löhneysen, and K. Samwer (With 1 Figure)	413
Time-Dependent Specific Heat of Vitreous Silica Between 0.1 and 1 K By W. Knaak and M. Meissner (With 3 Figures)	416
Phonon-Dispersion Measurements in Glasses. By M. Rothenfusser, W. Dietsche, and H. Kinder (With 3 Figures)	419

*invited paper

The Influence of Two-Level States on the Thermal Conductivity of Amorphous Materials. By D.E. Farrell, J.E. de Oliveira, and H.M. Rosenberg (With 2 Figures)	422
Low-Frequency Elastic Loss in Dielectric and Metallic Glasses at Low Temperature. By H. Tietje, M. v. Schickfus, E. Gmelin, and H.-J. Güntherodt (With 3 Figures)	425
Phonon Absorption Due to Two-Level Systems in Metallic Glasses By N. Thomas (With 1 Figure)	428
Resonant Interaction of Acoustic Waves with Two-Level Systems in a Fluorozirconate Glass. By R. Vacher, J. Pelous, M. Schmidt, P. Doussineau, and A. Levelut (With 2 Figures)	431
Heat Treatment Effects on the Phonon-Electron Contribution to Thermal Conduction in Amorphous $Zr_{70}Cu_{30}$. By P. Esquinazi and F. de la Cruz (With 2 Figures)	434
Disorder-Induced Light Scattering in α -AgI. By E. Cazzanelli, A. Fontana, G. Mariotto, V. Mazzacurati, G. Ruocco, and G. Signorelli (With 3 Figures)	437
Discussions	440

Part X Phonon Echoes

Rotary Phonon Echoes in Silica Glass. By B. Golding, D.L. Fox, and W.H. Haemmerle (With 2 Figures)	446
Pseudospin Echoes in Borate Glasses. By M. Devaud, J.-Y. Prieur, and W.D. Wallace (With 2 Figures)	449
The Enhancement of Phonon Echo Generation by Defects in Crystals By D.J. Meredith, H. Mkhwanazi, J.K. Wigmore, and T. Miyasato (With 2 Figures)	452
On Theory of Echo Phenomena in Amorphous Materials By V.S. Kuz'min and A.P. Sayko	455
Discussions	457

Part XI Spin-Phonon Interaction

Evidence for Phonon Scattering by Magnetic Two-Level Systems in Crystalline Spin-Glass $Eu_xSr_{1-x}S$. By C. Arzoumanian, B. Salce, A.M. de Goër, and F. Holtzberg (With 2 Figures)	460
Phonon Spectroscopy of MnF_2/ZnF_2 Mixed Crystals. By P.J. King, D.T. Murphy, and V.W. Rampton (With 2 Figures)	463
Heat Transport by Phonons and Magnons in Ferromagnetic EuS By G.V. Lecomte, H. v. Löhneysen, and W. Zinn (With 2 Figures)	466
Discussions	469
Index of Contributors	471

Part I

Acoustic Phonon Spectroscopy

Chairmen:

W. Dietsche K. Dransfeld T. Ishiguro G.A. Northrop

J. P. Wolfe A. F. G. Wyatt

Crossing Effects in Phonon Scattering

L.J. Challis

Department of Physics, University of Nottingham, University Park
Nottingham NG7 2RD, England

Resonant scattering from a phonon current can occur at the transition frequencies ν_i associated with the electronic or motional energy levels of impurity ions or centres present in the crystal. If the concentration of centres is 'small' the scattering will only be significant within a narrow frequency bandwidth Δ [1] which may be much less (≤ 1 GHz) than that of the phonon current ($\sim 2kT$ for a thermal current or ~ 40 GHz at 1K). Under these conditions the frequency spectrum of the phonon current has sharp holes burned in it as shown in fig. 1(a). In many cases these can be moved to and fro by applying an external perturbation such as a magnetic field. Sharp features in the total scattering occur when two of these holes cross ($\nu_i = \nu_j$) or in some cases anticross and these provide spectroscopic information which can be of quite high precision and resolution.

There are three main effects [2], frequency, level and anticrossing.

1. Frequency Crossing

This effect only requires that 2 transition frequencies become equal. It was first observed and accounted for qualitatively by BERMAN et al. [3] using the heuristic model illustrated in fig. 1(b) which assumes that when resolved, the 2 resonant processes completely block the 2 rectangular conduction channels shown shaded. However, when they are crossed only one channel is blocked so the total conduction rises giving a signal $\Delta K/K_0 \sim$ channel conduction/total conduction and width \sim channel width. In practice of course a channel is never entirely blocked. Its conduction depends on $\tau(\nu)$, the phonon relaxation time and $\tau(\nu) = (\tau_B^{-1} + \tau_1^{-1} + \tau_2^{-1})^{-1}$, where τ_B^{-1} , τ_1^{-1} and τ_2^{-1} are respectively the background and two resonant scattering rates. Expansion of $\tau(\nu)$ contains functions of the product $\tau_1^{-1}\tau_2^{-1}$ which is essentially zero at all frequencies when the two processes are resolved, but becomes non-zero for $\nu \sim \nu_1 = \nu_2$ when the processes are crossed [Fig 2]. So the crossing signal is a consequence of the non-linear dependence of $\tau(\nu)$ on the scattering rates.

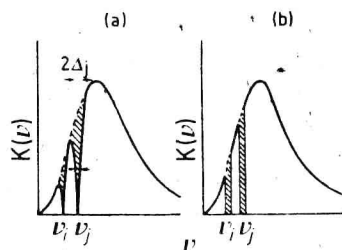


Figure 1

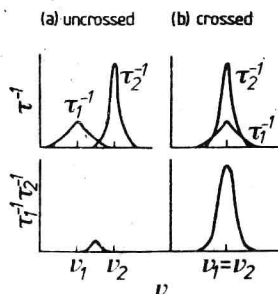


Figure 2

At low temperatures and in a Debye model the conductivity differs from that of the pure crystal by

$$\Delta K = K_0 - K = CT^3 \int_0^{\infty} \frac{x^4 e^x}{(e^x - 1)^2} \left[\tau_B - \tau(\nu) \right] d\nu \text{ where } x = h\nu/kT.$$

In general the crossing signal $\Delta W/W_0 \approx -\Delta K/K_0$ ($W = 1/K$) can be computed from τ_1^{-1} and τ_2^{-1} by calculating ΔK as a function of the separation of the 2 frequencies in the region of the crossing frequency ν_0 . However, when the holes have widths $\ll kT$, we can simplify the calculation since

$$\Delta K \approx CT^3 \left[\frac{x^4 e^x}{(e^x - 1)^2} \right]_{\nu_0} \int_0^{\infty} \left[\tau_B - \tau(\nu) \right] d\nu. \text{ Indeed in some}$$

limits the integral can be solved analytically for both Lorentzian and Gaussian line shapes giving simple expressions for the form of the signal [4]. So the size and shape of frequency crossing signals can provide information on the resonant scattering rates and hence the spin-phonon coupling constants or, if these are known, on the ionic concentrations. Their positions can provide spectroscopic information such as the spin-Hamiltonian parameters. Although this discussion refers to steady heat currents, similar analysis of course applies to heat pulses.

An example of a frequency crossing signal is shown in fig. 4 at low resolution. The signal shows the change in temperature difference along a sample as the field is swept and is usually displayed at $\Delta W/W_0$. The system is V^{3+} in Al_2O_3 whose levels for $B \parallel c$ axis correspond to those of fig. 3 and give rise to a crossing at a field $B = D/3g_{11}\beta$. The crossing moves to higher fields when these are moved away from the c axis, and D and g_{\perp} can be obtained rather accurately from the straight line plot of B^{-2} against $\cos^2\theta$ (θ is the angle to the c axis) if g_{11} is known from EPR which is very often the case in such systems [5].

The upper 2 levels of fig.3 are in fact each split into 8 by hyperfine interaction, as shown in fig.[3]. This gives rise to the structure shown in fig. [5], [7]. Figure 6 shows the differential of this signal obtained by applying a small modulation field to the sample [8].

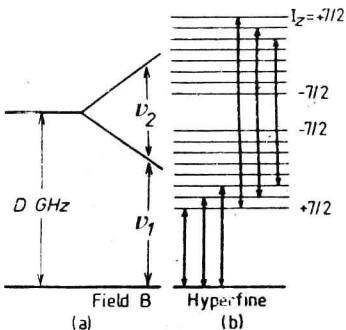


Fig.3: the energy levels of V^{3+} in Al_2O_3 . If we neglect hyperfine splitting ($\sim 10^{-3}D$), $v_1 = D - g_{11}\beta B$ and $v_2 = 2g_{11}\beta B$ so $v_1 = v_2$ when $B = D/3g_{11}\beta$

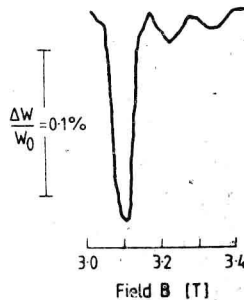
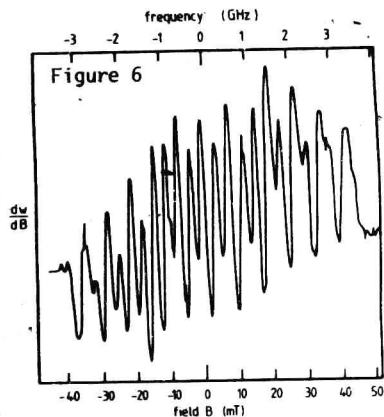
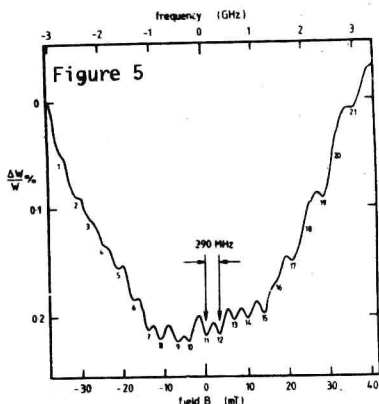


Fig 4: shows the frequency crossing signal of fig 3 displayed at low resolution. The 2 signals at higher fields are due to V^{3+} pairs present at a concentration $\sim 10^{-2}$ ppm [6]



In this case and many others that have been reported the 2 scattering processes were both from the same type of ion but crossing signals have also been seen when the processes are from 2 ions in inequivalent sites [3], an ion and an ion pair [6] and 2 entirely different ionic species [9], [10]. So, as WALTON first stressed [9] one can use a known ion as a probe to investigate another and the fact recently demonstrated that they do not have to be in the same part of the sample opens up the scope of the technique.

2. Frequency Crossing between spatially separated Ions

This has been demonstrated [11] using an Al_2O_3 bicrystal doped with Fe^{2+} ions in one half and V^{3+} in the other [Fig.7]. Several crossings occur between the transition frequencies of the two ions and fig. 7 shows two of these (lines C and D). The increase in their size when heat injection is switched from H_V to H_{Fe} shows that the Fe^{2+} holes in the phonon current are carried across the interface; the V^{3+} ions have little effect on this current when tuned to a hole. This technique seems capable of being developed in various ways and we hope to use it to study ions in epitaxial and diffused layers, electrons in inversion layers, etc. by crossing their frequencies with those of probe ions in the bulk crystal [12].

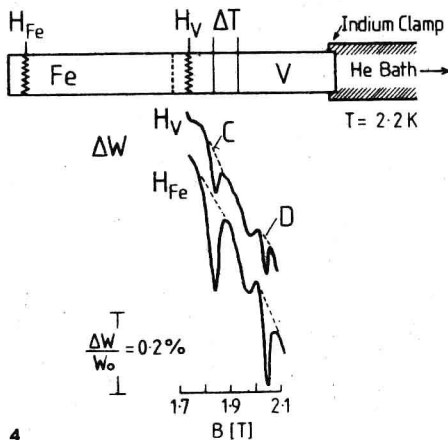


Figure 7: shows frequency crossing signals from the Fe/V Al_2O_3 bicrystal shown in the upper part of the figure. The signals ΔW are minima in the temperature difference on the V-doped half. The signals are ~ 3 times larger when heat is injected at H_{Fe} rather than at H_V in the control experiment when the signals are due to traces of Fe^{2+} in the V half

3. Level Crossing

The effects that should be observable here using phonons are analogous to the HANLE effect seen in light scattering in 1924 [13] and first explained by BREIT in 1933 [14]. In recent years it has been used as a technique for high resolution spectroscopy [15]. Suppose an ion has 2 crossing levels with energies $h\nu_1$ and $h\nu_2$ above a singlet ground state and that the upper 2 levels can be made to cross by a magnetic field (fig.8(a)) making $\nu_1 = \nu_2$. If white light is incident on the ion, a photomultiplier can be used to measure the total intensity I_T of the components at ν_1 and ν_2 scattered into a particular small solid angle. Now if $|\nu_1 - \nu_2| \gg \gamma$ (γ is their combined line width), $I_T = I(\nu_1) + I(\nu_2)$ but if $|\nu_1 - \nu_2| \lesssim \gamma$, interference takes place in the emission process and $I_T = |A(\nu_1) + A(\nu_2)|^2 = I_1 + I_2$ plus an interference term. So the photomultiplier records a signal of width γ at the crossing point. There seems no reason to suppose that similar effects should not occur with phonons although so far as I know, no experiments have been reported. It might be possible to see them in thermal conduction which would certainly be affected by changes in the angular distribution of the scattered phonons that occur at a level crossing. However, at the concentrations used in phonon experiments so far, these changes would be accompanied by frequency crossing effects and while the resulting signal would certainly differ from a pure frequency crossing signal [16], it is not clear whether these differences could be identified. So although it would seem that it would be interesting to explore these effects in this way, experiments looking more directly at the angular distribution would seem to be more promising.

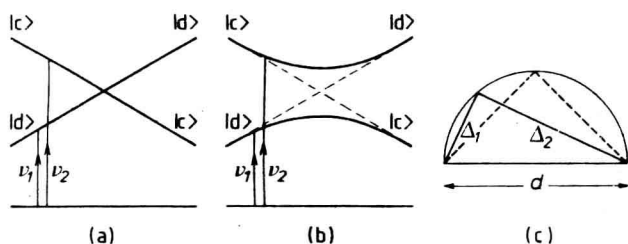


Figure 8

A complication in level crossing experiments comes from the effect of random strain which may prevent levels from approaching to within their linewidths (anticrossing).

4. Anticrossing

If there is coupling between the 2 approaching levels of fig.8(a), they will repel each other or anticross as shown in fig.8(b). So if the holes in the heat current at ν_1 and ν_2 are narrower than their nearest separation, they can never overlap and no frequency crossing signal can occur. However, there can still be another sort of signal because of the state mixing that occurs at the anticrossing. This changes the widths Δ_1 , Δ_2 of each of the holes while keeping $\Delta_1^2 + \Delta_2^2$ constant. The additional thermal resistance caused by the existence of the holes $\propto (\Delta_1 + \Delta_2)$ which has a maximum at the centre of the anticrossing when the 2 hole widths become equal ($\Delta_1 = \Delta_2$). This can be seen in Fig 8(c) where $\Delta_1^2 + \Delta_2^2 = d^2$ (d = diameter of semicircle).